



Comparative assessment and optimization of Pb(II), Ni(II), and Zn(II) biosorption onto *Gelidella acerosa* in single systems: equilibrium and kinetic modeling

J. Vijayaraghavan^{a,*}, D. Zunaithur Rahman^b, J. Thivya^c

^aDepartment of Civil Engineering, University College of Engineering Ramanathapuram, Ramanathapuram – 623 513, Tamil Nadu, India, Tel. +91 94885 28279; email: drjvr1988@gmail.com (J. Vijayaraghavan)

^bDepartment of Civil Engineering, Mohamed Sathak Engineering College, Kilakarai – 623 806, Tamil Nadu, India, Tel. +91 80123 36482; email: zunaithur@gmail.com (D. Zunaithur Rahman)

^cDepartment of Civil Engineering, University College of Engineering Dindigul, Dindigul – 624 622, Tamil Nadu, India, Tel. +91 94426 45058; email: thivyame@gmail.com (J. Thivya)

Received 9 March 2020; Accepted 20 August 2020

ABSTRACT

A study was conducted to remove metal ions of Pb(II), Ni(II), and Zn(II) from the aqueous solution by using red seaweed *Gelidella acerosa* in different environmental conditions. Biosorption of metal ions was observed with varying factors such as pH (2–9), seaweed dosage (2–10 g/L), initial metal concentration (10–125 mg/L), and contact time (0–300 min). To evaluate the element analysis and properties of seaweed, atomic absorption spectroscopy, Fourier-transform infrared, scanning electron micrographs (scanning electron microscopy-energy dispersive X-ray spectroscopy), Brunauer–Emmet–Teller were used. *G. acerosa* recorded a metal uptake of 73.99, 87.82, and 127.08 mg/g, respectively, for Pb, Ni, and Zn ions at optimum pH (5, 2, and 8 for Pb, Ni, and Zn), seaweed dosage (2 g/L) and initial metal concentration (100 mg/L) equilibrium at 120 mins. The kinetic model data obtained at various initial Pb, Ni, and Zn concentrations showed that the biosorption rate was quick, while the data were modeled successfully with the pseudo-first and pseudo-second-order. To describe metal ions isotherm data, the different models of Langmuir, Freundlich, and Redlich–Peterson and Sips were used, and the Sips model portrayed the high-correlation isotherm data.

Keywords: Wastewater; Biosorption; Pb, Ni and Zn; Metal, *Gelidella acerosa*; Red seaweed

1. Introduction

Water is an essential resource for all living beings in the world. It is the duty and responsibility of every human being to protect it safely for the next generation. Since the need for resource and raw materials are increasing abruptly, the industries are getting developed day by day. The major water bodies affected by wastewater directly or indirectly discharged from industries in the form of organic and inorganic chemicals [1–3]. We could take some remedial measures to control because of pollutants are highly soluble and difficult to separate. Even though laws and regulations are

existing, still so many industries are discharged high-level hazardous pollutants without adequate treatment [4–6]. Industrial wastewater contains metals mixed with the environment and is of both natural and industrial activities. The natural activities are volcanic explosion, weathering, erosion of minerals, and rocks, etc. Industrial activities are metal plating, leather, textile industries, pesticides, and fertilizers, manufacturing batteries, paint and pigment, electrical appliances, and chemical industries, etc. [7–9].

These heavy metals are creating highly hazardous health issues for living tissues of all living things either

* Corresponding author.

through the direct intake or food chain, even if the metals exist in low concentration. Even some metals are required for most of the living organisms for the proper function of the body and surplus intake causes toxicity [10,11]. Due to the high-level toxins, bioaccumulation, biomagnification, non-biodegradability, and carcinogenic in nature of pollutants, it creates a variety of diseases and disorders and may lead to cancer to human beings. The high-level toxicity gives physical discomfort, life-threatening illness, high blood pressure, aggressive behavior, increased allergic reaction, and autoimmune diseases [12]. United states environmental pollution Agency (USEPA) and world health organization (WHO) has listed out as lead (Pb), nickel (Ni), zinc (Zn), etc., are potentially dangerous and affect the growth of metabolism of cells in all living beings [13,14].

Researchers are facing a tough task of cost-effective treatment to develop good performance, disposal, and replace the costly wastewater treatment methods such as membrane separation, reverse osmosis, ion-exchange, electro flotation and dialysis, chemical precipitation, and coagulation, etc. [15]. Research articles show that membrane filtration, adsorption, and ion exchange are the most frequently studied in the treatment of heavy metals. Except for adsorption, other methods are associated with low efficiency, high instrumental and operational costs, impractical for large scale, and produce large quantity of sludge [16,17]. Adsorption is acknowledged as attracting the attention of researchers as physico-chemical treatment processes that are found to be the simplest, safest, most viable, and most efficient in heavy metal removal. This method is comparatively different and new as an interaction between living, non-living, and metallic ions within a single system. Its process involves the separation of a substance from one phase and its accumulation at another surface [18]. The advantages of this method are unproblematic design and fewer requirements of control systems, economical, and absence of toxic sludge, metal selectivity, and recovery, suitable and effective even at low concentrations [19].

Adsorbent should have a large surface area, easy accessibility, cost-effective with environmental friendliness, simple processing procedures, low solubility, high adsorption capacity, ease of regeneration, quick separations, favorable thermal, chemical, mechanical stability, and kinetic characteristics [3]. The adsorption capacity of a biosorbent is influenced by pH, dosage, temperature, initial concentration, contact time, and temperature [20]. Seaweed is a pleasant renewable biosorbent with more than a thousand seaweed species that grow in the aquatic environment and economically feasible without any cultivation demands. It is growing faster and has a higher rate of CO₂ fixation relative to land-planted crops [21]. *Gelidiella acerosa* is macro red marine seaweed, abundantly growing in coastal areas of south India. It has been used as a gelling agent to make agar, stabilizer agents in food, pharmaceutical, and biotechnological industries and valuable antioxidants for treating reactive oxygen species (ROS) mediated diseases and gastrointestinal disorders [22,23]. But the application of *G. acerosa*'s in biosorption of metal is very much limited. In this study, the *G. acerosa*'s is used as an adsorbent for the biosorption of three different metals namely Pb(II), Ni(II), and Zn(II) in the batch adsorption process. As per EPA

Notification: GSR 176 (E), April 02, 1996, the tolerance limit of Pb(II), Ni(II), and Zn(II) disposal into the environment is 0.1, 3, and 5 mg/L, respectively. The kinetics and equilibrium isotherms of the *G. acerosa* have been developed and analyzed with various models of adsorption.

2. Materials and methods

2.1. Adsorbent preparation

Geliedella acerosa (GA) was collected from Kurusadai island beaches, Mandapam, Tamilnadu, India (9°14'N 79°12'E). To remove impurities, the collected seaweed was washed several times with deionized water (DI). The washing process continued until the pH of the DI water was equal to the pH of the washing solution. The washed seaweed was then completely dried for 10 d in sunlight. The dried seaweed was incurred for 6 h at 105°C, cut into small pieces, and pulverized using a domestic mixer (1 HP Micro active, India). In this study, dry biomass in the range of particle sizes 150–175 μm was used without chemical pretreatment for sorption experiments.

2.2. Chemicals and stock solution

The stock solution containing 1,000 mg/L of Pb(II), Ni(II), and Zn(II) was prepared by dissolving the required amount of AR Grade PbSO₄, NiSO₄·6H₂O, and ZnSO₄·7H₂O in DI water. The initial required concentration of metal ion standards was prepared by diluting the above stock solution appropriately. All analytical grade chemicals obtained from MERCK (Delhi).

2.3. Adsorption experiment

On the batch scale experiments carried by using GA seaweed to remove the metal ions from the known concentration of aqueous solutions. Using 0.1 M HCl or 0.1 M NaOH, the metal ion solution pH was originally adjusted to the required value. For each 100 mL solution, 0.6 g of marine seaweed was added in a 250 mL volumetric flask. The mixture was agitated on the rotary shaker at 150 rpm for 5 h at 30°C. After the biosorption process, the content of the beakers was centrifuged at 4,000 rpm for 3 min. The supernatant of the solutions was analyzed for residual metal ion concentration using atomic absorption spectroscopy (AAS vario 6, Analytik Jena, Germany). All experiments were tripled and the average values were reported. Kinetic experiments were carried out in the same way, except that the samples were taken at predetermined intervals of time.

2.4. Isotherm and kinetic studies

The number of metal ions sorbed by *G. acerosa* was calculated using the following equation from the variations between the original quantity of metal ions added and the quantity remaining in the supernatant:

$$\text{Adsorbent capacity (Q)} = \frac{V(C_0 - C_f)}{M} \quad (1)$$

$$\text{Adsorbent efficiency (\%)} = \left[\frac{(C_0 - C_f)}{C_0} \right] \times 100 \quad (2)$$

where Q is the uptake of metal ions (mg/g), C_0 and C_f are the original and final concentrations of metal ions in the solution (mg/L), V is the volume of metal solution (L), respectively, and M is the weight of added seaweed (g).

Four isotherm models have been used to define the experimental data of metal ions as follows:

$$\text{Langmuir model: } Q = \frac{Q_{\max} b_L C_f}{1 + b_L C_f} \quad (3)$$

$$\text{Freundlich model: } Q = K_F C_c^{1/n_F} \quad (4)$$

$$\text{Redlich–Peterson model: } Q = \frac{K_{RP} C_f}{1 + \alpha_{RP} C_f^{\beta_s}} \quad (5)$$

$$\text{Sips model: } Q = \frac{K_s C_f^{\beta_s}}{1 + \alpha_s C_f^{\beta_s}} \quad (6)$$

where Q_{\max} is the maximum metal uptake (mg/g), b_L is the Langmuir equilibrium coefficient (L/mg), K_F is the Freundlich coefficient (L/g)^{1/n_F}, n_F is the Freundlich exponent, K_{RP} is the Redlich–Peterson isotherm coefficient (L/g), α_{RP} is the Redlich–Peterson isotherm coefficient (L/mg)^{β_s}, and β_s is the Redlich–Peterson model exponent, K_s is the Sips model isotherm coefficient (L/g)^{β_s}, α_s is the Sips model coefficient (L/mg)^{β_s}, β_s is the Sips model exponent [24–26].

Two kinetic models were used to represent experimental data from metal ions biosorbents in the kinetics:

$$\text{Pseudo-first-order model: } Q_t = Q_e (1 - \exp(-k_1 t)) \quad (7)$$

$$\text{Pseudo-second-order model: } Q_t = \frac{Q_e^2 k_2 t}{1 + Q_e k_2 t} \quad (8)$$

where Q_e is the amount of metal ions biosorbed at equilibrium (mg/g), Q_t is the amount of metal ions biosorbed at time t (mg/g), k_1 is the pseudo-first-order rate constant (1/min), and k_2 is the pseudo-second-order rate constant (g/mg min). All model parameters were assessed using Sigma Plot (V4.0, SPSS, USA) software by non-linear regression [24–26].

Fourier IR spectrometer transform (Perkin Elmer, Spectrum RX1) was used to observe the type of functional groups in biosorbent responsible for metal adsorption in sorbent IR spectral studies (4,000–400 cm⁻¹). The samples were made using KBr in the form of pellets. Scanning electron micrographs (SEM) were taken for fresh and metal loaded algae. Dried biosorbent samples were attached to a stub, covered with platinum in an auto-fine coater (JEOL JFC 1600 Japan) and scanned with an electron scanning microscope (JEOL JSM 6360 Japan). The pore diameter, pore radius, and surface area were determined by the multipoint Brunauer–Emmett–Teller analyzer (Autosorb iQ Station 1).

3. Result and discussion

3.1. Effect of solution pH

Metal ion interaction with biosorbent is a combined result of metal charges and the biosorbent surface. The pH solution is an important environmental parameter that affects the sorption behavior of the solution on the biosorbent surface that controls the biosorption process efficiency [27,28]. The acidity of the solution affects the competition between the hydrogen ions and metal ions for the active sites present on the surface of the biosorbent [29]. The impact of pH on *G. acerosa*'s biosorption of Pb(II), Ni(II), and Zn(II) was explored over a pH spectrum of 2–9 in the aqueous solution and the outcomes are outlined in Fig. 1. The efficiency of metal ion removal in batch mode (initial metal concentration of 100 mg/L, adsorbent dose of 6 g/L, and agitation rate of 150 rpm) increased significantly from pH 2 to 5 in Pb(II) and from pH 2 to 8 in Zn(II), while gradually decreased from 2 to 9 in Ni(II). The results verified that the pH heavily affected metal removal. The pH influences both the biosorbent material's surface charge and metal ionization. Pb(II) biosorption increased from 3.98 mg/g at pH 2–15.40 mg/g at pH 5, Ni(II) gradually decreased by 13.93 mg/g at pH 2 to 1.24 mg/g at pH 9, and Zn(II) increased by pH 2–8 from 3.74 mg/g. The highest efficiency of metal ion sequestration was achieved at pH 5, 2, and 8, respectively (92.42% for Pb, 83.59% for Ni, and 92.67% for Zn). Then the removal effectiveness was decreased by raising the pH to 9. The functional groups present on the *G. acerosa* cell layer (hydroxyl and carboxyl) will be protonated by H⁺ electrons at acid pH levels owing to the existence of surplus H⁺ electrons in water and overall positive charges [30,31]. On the other hand, metal releases positively charged ions into a solution that shows the negatively charged cell surface with electrostatic attraction. Due to the positive overall biomass charge under strong acid conditions, the electrostatic attraction of metal ions is lower and therefore relatively lower absorption was observed [32,33] (Fig. 1). As the pH increases, the concentration of H⁺ electrons reduces and *G. acerosa*'s binding sites by electrostatic attraction occupy more metal ions. Comparing the extent of removal efficiency, Pb(II) = Zn(II) > Ni(II) by using this red seaweed *G. acerosa*.

3.2. Effect of sorbent dosage

The effect of seaweed dosage on metal ion removal was investigated by varying adsorbent dosage from 2 to 10 g/L in an aqueous solution shown in Fig. 2 (optimum pH, initial metal concentration 100 mg/L, and agitation speed 150 rpm). It has been observed from the analysis of the experimental data obtained for *G. acerosa* red algal biomass that the efficiency of removal of Pb(II), Ni(II), and Zn(II) decreases with the increase in the dosage of seaweed. For example, *G. acerosa*'s metal removal efficiency fell from 93.28% to 79.50% for Pb, from 90.98% to 59.68% for Ni and 95.75% to 56.83% for Zn, respectively, when biomass dosage increased from 2 to 10 g/L. The observed decrease in removal efficiency with a decrease in the dosage of seaweed may be due to a decrease in the number of possible functional groups and seaweed biomass surface area. On the other side, when the seaweed dosage increases,

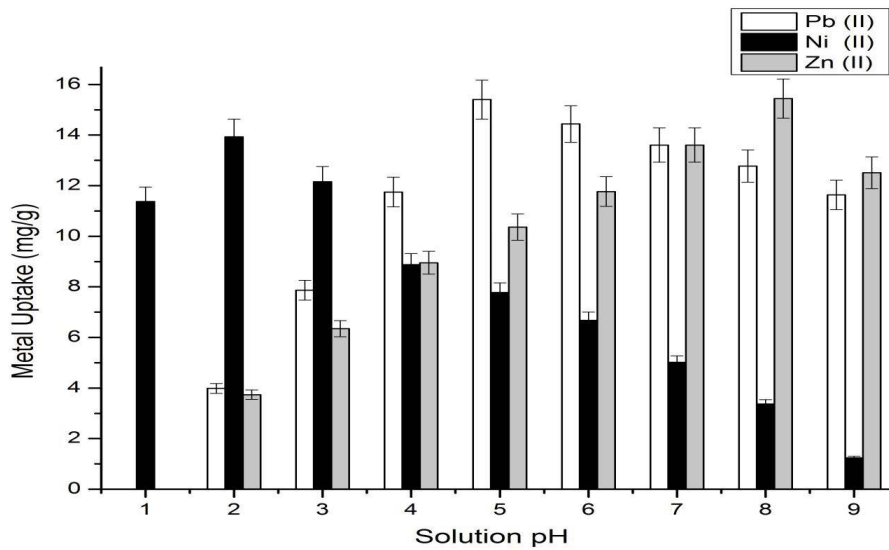


Fig. 1. Effect of solution pH during Pb(II), Ni(II), and Zn(II) biosorption onto *G. acerosa*.

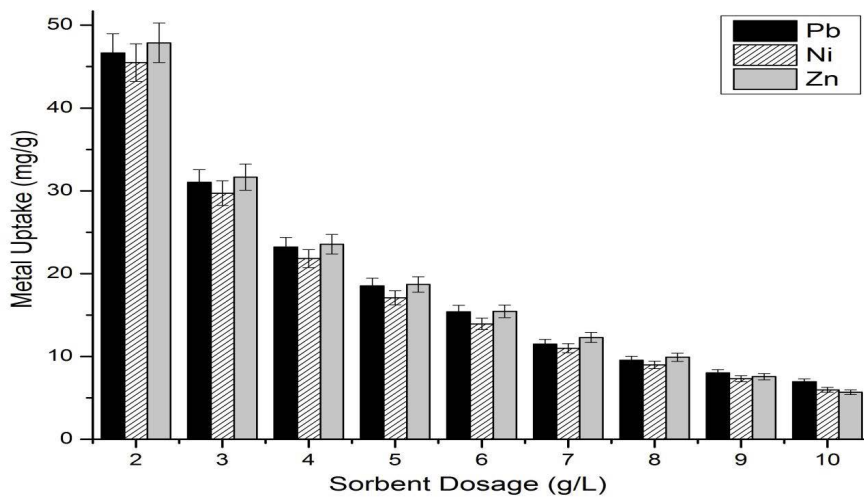


Fig. 2. Effect of sorbent dosage during Pb(II), Ni(II), and Zn(II) biosorption onto *G. acerosa*.

the metal uptake reduces [34,35]. For example, *G. acerosa*'s metal uptake capacity decreased from 46.64 to 6.95 mg/g for Pb(II), 45.49 to 5.97 mg/g for Ni(II) and 47.88 to 5.68 mg/g for Zn(II) when the biomass dosage increased from 2 to 10 g/L, respectively. The accessible metal ions are greater than the number of binding locations at small sorbent dosages, hence the absorption is greater. On the contrary, the available metal ions are insufficient at high biosorbent dosages to cover all the exchangeable sites on the biosorbent seaweed, usually resulting in low metal absorption [36,37]. Comparing the percentage of sequestration and sorption uptake values Zn(II) > Pb(II) > Ni(II), 2 g/L algal dosage was chosen as the optimum for further studies for three metals.

3.3. Functional group spectra and surface analyses of *G. acerosa*

FT-IR analyzes on *G. acerosa* biomass loaded with raw and metal were conducted to know the nature of the

functional groups associated with metal biosorption. The raw *G. acerosa* FT-IR spectrum, showing the complicated nature of biomass examined before and after metal ion adsorption, showed several absorption peaks, as demonstrated in Fig. 3. As shown in Table 1, *G. acerosa* may be assigned certain unique peaks. After exposure to Pb, Ni, and Zn metal ions, significant alterations in the functionalities of seaweed (Fig. 3) were noted. This is mainly because binding groups have been involved when in contact with metal ions, and thus the wavenumbers have changed. In the metal charged *G. acerosa* with asymmetric and symmetric C=O stretches and C–O stretches (Table 1) significant changes have been observed in specific cases. These results confirm that negative binding groups occur during the biosorption of metal ions on the *G. acerosa* surface.

Raw and metal sorbed *G. acerosa* morphological structure was examined using a SEM (Fig. 4). Before adsorption, it can be visualized both the surface with an uneven

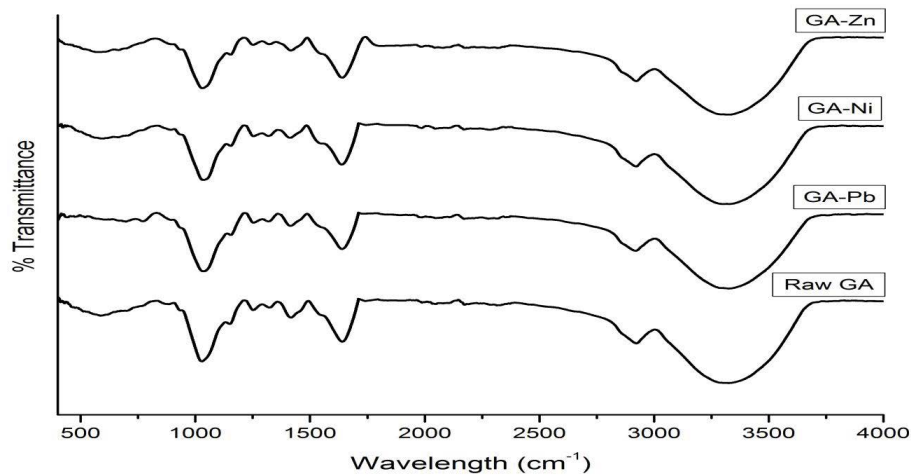


Fig. 3. FT-IR spectra of raw GA and metal loaded GA.

Table 1
Frequencies recorded in raw and metal loaded *G. acerosa*

Functional group	Wavenumber (cm ⁻¹)			
	Raw GA	Pb loaded GA	Ni loaded GA	Zn loaded GA
–OH, –NH stretching	3,325.64	3,326.61	3,325.64	3,329.50
Asymmetric CH ₂ stretching	2,922.69	2,918.73	2,921.63	2,922.69
–P–H– group	2,315.12	2,278.48	2,285.23	2,317.05
Asymmetric C=O stretch of COOH	1,641.13	1,641.13	1,639.20	1,640.16
Symmetric C=O	1,416.46	1,415.49	1,413.57	1,416.46
C–O (COOH) stretching	1,252.54	1,253.50	1,253.50	1,251.58
C=C stretching	1,149.37	1,154.19	1,154.19	1,153.22
C–O (alcohol) band	1,027.87	1,033.66	1,034.62	1,029.80
C=O of aromatic stretching	883.34	772.35	–	–
Alkane group	685.29	697.14	595.90	684.33

morphology and the soft surface. The metal biosorption mechanism coincided with SEM pictures as an electrostatic interaction of the negatively loaded surface of the seaweed with the positive metal ions. *G. acerosa* surfaces were coated with Pb, Ni, and Zn ions relatively flat and smooth. The SEM images of *G. acerosa* show protruding surfaces and microstructures due to the deposition of Ca, K, and other crystalloids in salt. An assessment by energy-dispersive X-ray spectroscopy (EDS) disclosed that raw *G. acerosa* was made up of significant compositions of oxygen (88%), potassium (3.09%), and sulfur (2.28%). Brunauer–Emmett–Teller (BET) analysis showed that better surface area (1.712 m²/g), pore volume (1.558 × 10⁻³ cm³/g), and pore radius (1.82 nm) of GA and influence in adsorption capacity.

3.4. Biosorption isotherm and modeling

The adsorption isotherm is used to explain the relationship between the amount of metal ions in the solution to the amount of metal ions on to the biosorbent [38]. Experimental metal biosorption isotherms produced for *G. acerosa* at pH 5, 2, and 8 correspondings to Pb(II), Ni(II), and Zn(II) are

shown in Fig. 5. Each of these isotherms could be considered as a partially straight line, that is, the ratio between the metal concentration in the solution and the biosorbed concentration on the *G. acerosa* decreases with an increase in the concentration of metal, providing a strict plateau with a concave curve [39]. Zinc has a high uptake of 58.95 mg/g compared to lead (56.79 mg/g) and nickel (54.76 mg/g).

For the evaluation of experimental metal isotherm data, several two- and three-parameter models were used. Due to outstanding *R*² values, the Langmuir model is applied to the experimental metal isotherm data. For monolayer adsorption on a surface consisting of a limited amount of identical locations, the Langmuir isotherm is applicable [40,41]. The Langmuir constant, *Q*_{max}, is the maximum metal uptake values that the system can achieve. By contrast, *b*_{*L*} is the affinity between the biosorbent and the sorbate. In comparison with Ni(II) and Zn(II) (Table 2), both constants (*Q*_{max} and *b*_{*L*}) were observed to be maximum for Pb(II). Since the Langmuir isotherm model can predict any biosorbent's maximum biosorption capacity under controlled conditions, it is possible to compare the sorbent performance to the particular metal. Initially empirical, the Freundlich isotherm

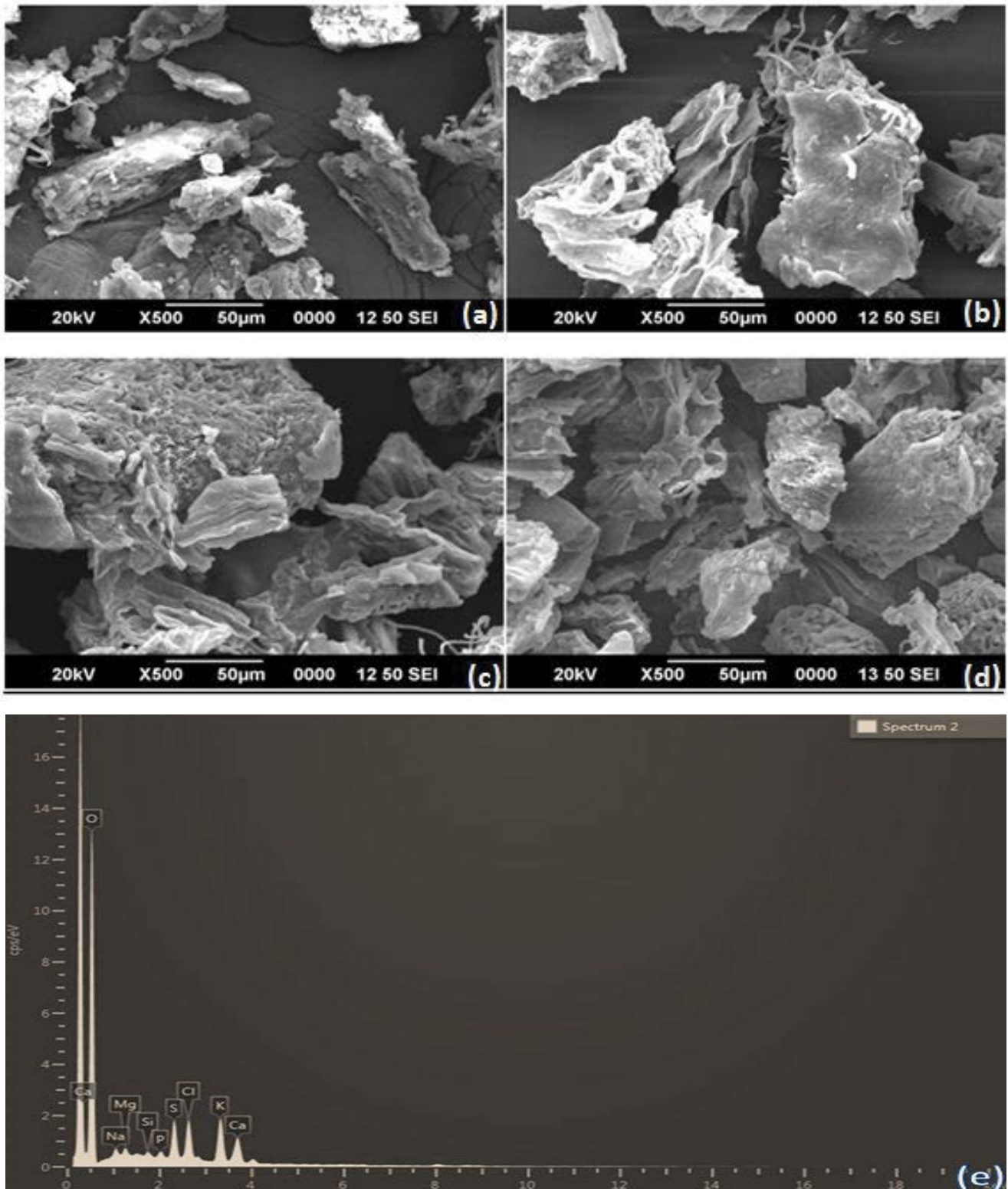


Fig. 4. SEM images of (a) raw GA, (b) Pb loaded GA, (c) Ni loaded GA, (d) Zn loaded GA, and (e) SEM-EDS of raw GA.

was later viewed as sorption of heterogeneous surfaces or surfaces that support sites of variable affinities. It is assumed that stronger functional groups are first occupied and that binding power is reduced by increasing site occupancy [42].

It was obvious from the results (Table 2) that Zn(II) and Pb(II) had elevated values of K_f and $1/n_f$ compared to Ni(II). This means that *G. acerosa* has the highest binding ability and a strong affinity between biomass and metal ions (Zn and Pb)

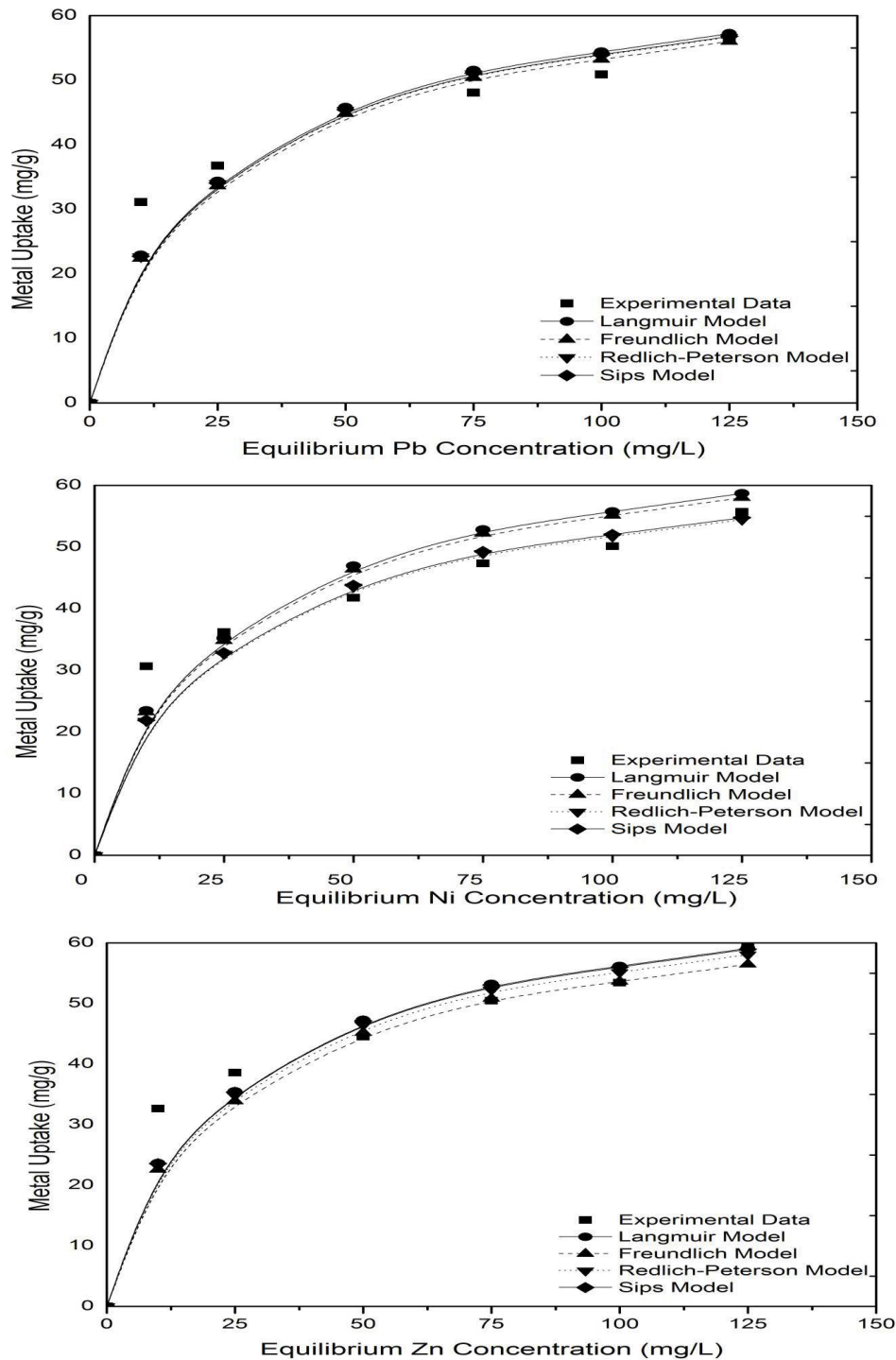


Fig. 5. Biosorption isotherm of Pb(II), Ni(II), and Zn(II) onto *G. acerosa*.

has also been found. However, as comparatively small R^2 values were observed, the description of the experimental data in the Freundlich model was not adequate (Table 2).

In this study, the Redlich–Peterson model (three-parameter) was used to enhance the prediction of metal isotherm data. This model includes in a single equation the features of both the Langmuir and Freundlich models and indicates an adsorption scheme as hybrid and does not

follow suitable monolayer adsorption [43]. As expected, the Redlich–Peterson model described metal isothermic data with great accuracy (Table 2). For all constants of the model, maximum values for *G. acerosa* were observed. The exponent of Redlich–Peterson was close to unity, confirming that more of the Langmuir type was the metal isotherm. The Sips model has also been used to describe metal isotherms generated for three metals. Sips isotherm is a

blended technique developed to predict heterogeneous procedures by Langmuir and Freundlich equations. The Sips model exponent (β_s) suggests the scheme's heterogeneity, that is, powerful system heterogeneity is indicated by the greater value of β_s . The model of Sips reduces at low rates to Freundlich, while the model of Langmuir predicts at high levels [44]. Table 2 indicates that β_s values were closer or greater than unity; this demonstrates that there were more Langmuir and heterogeneity in the present system.

For all the isothermic information examined (Table 2), applications of the Sips system led to high R^2 values.

Table 2
Isotherm model parameters during biosorption of Pb(II), Ni(II), and Zn(II) onto *G. acerosa*

Models	Constants	GA-Pb	GA-Ni	GA-Zn
Langmuir	Q_{max}	73.995	87.822	127.802
	b_L	0.262	0.122	0.139
	R^2	0.997	0.994	0.951
Freundlich	K_F	16.225	10.902	16.346
	n_F	0.574	0.666	0.740
	R^2	0.950	0.965	0.799
Redlich–Peterson	K_{RP}	18.986	9.497	15.701
	α_{RP}	0.250	0.052	0.040
	β_{RP}	1.002	1.279	1.625
	R^2	0.997	0.990	0.955
Sips	K_S	19.182	10.179	21.253
	β_S	0.972	1.154	1.133
	a_S	0.248	0.145	0.279
	R^2	0.998	0.996	0.993

The isotherm curves are shown in figures as expected by all four isotherm models.

3.5. Kinetics and modeling

Biosorption of Pb, Ni, and Zn on *G. acerosa* was researched within 5–300 min of contact time. The initial metal concentration at an optimum pH of three metal ions ranged from 10 to 125 mg/L was investigated. In Fig. 6, the metal biosorption profile was provided at different time intervals. For *G. acerosa*, about 96% for Pb(II), 91% for Ni(II), and 94% for Zn(II) removal was happened within 60 min for 100 mg/L metal ion concentration. This fast uptake of Pb, Ni, and Zn uptake is owing to the accessibility of surplus empty sites [45]. As the sorption advances, binding sites are occupied and fewer empty sites are rendered accessible on the adsorbent surface resulting in a reduction in sorption speed as shown in Fig. 6. The process achieved the equilibrium state after 120 min where there was no major shift in the metal solution as the metal ions occupy the available binding sites. With a rise in initial metal concentration, the time required to achieve equilibrium attainment (Fig. 6). In particular, it was discovered that the equilibrium contact time on red seaweed *G. acerosa* for metal ion biosorption was 300 min. It's obvious from Fig. 6, that the rise in the initial metal concentration enhanced *G. acerosa's* metal absorption capacity. A greater initial metal concentration was recognized as having a higher driving power to transport ions from the solution to the cell layer, leading in quicker removal and greater ability for adsorption [46]. To raise the initial metal concentration from 10 to 125 mg/L, *G. acerosa's* adsorption capacity increases from 4.96 to 63.62 mg/g for Pb(II), 4.85 to 62.67 for Ni(II), and 4.99 to 66.78 mg/g for Zn(II), respectively.

Table 3
Kinetic model parameters during biosorption of Pb(II), Ni(II) and Zn(II) onto *G. acerosa*

Metals	Model	Constants	10 mg/L	25 mg/L	50 mg/L	75 mg/L	100 mg/L	125 mg/L
Pb(II)	Pseudo-first-order	Q_e (mg/g)	4.9631	12.4005	25.2084	38.5613	51.3040	63.6188
		k_1 (1/min)	0.0602	0.0587	0.0565	0.0545	0.0526	0.0509
		R^2	0.9988	0.9989	0.9988	0.9984	0.9976	0.9966
	Pseudo-second-order	Q_e (mg/g)	5.0123	12.7029	26.4088	41.2517	55.9680	70.6875
		k_2 (g/mg min)	0.0662	0.0125	0.0040	0.0020	0.0012	0.0009
		R^2	0.8590	0.9607	0.9873	0.9904	0.9856	0.9832
Ni(II)	Pseudo-first-order	Q_e (mg/g)	4.8470	12.1053	24.6047	37.6336	50.0390	62.6715
		k_1 (1/min)	0.0456	0.0447	0.0432	0.0418	0.0405	0.0392
		R^2	0.9931	0.9934	0.9937	0.9937	0.9935	0.9930
	Pseudo-second-order	Q_e (mg/g)	4.8950	12.4005	25.7763	40.2592	54.5880	69.6350
		k_2 (g/mg min)	0.0341	0.0064	0.0023	0.0013	0.0009	0.0007
		R^2	0.9082	0.9856	0.9930	0.9922	0.9910	0.9908
Zn(II)	Pseudo-first-order	Q_e (mg/g)	4.9874	12.4599	25.3313	38.7505	52.6625	66.7834
		k_1 (1/min)	0.0525	0.0513	0.0495	0.0478	0.0463	0.0448
		R^2	0.9972	0.9972	0.9970	0.9964	0.9956	0.9945
	Pseudo-second-order	Q_e (mg/g)	5.0368	12.7638	26.5375	41.4541	57.4500	74.2038
		k_2 (g/mg min)	0.0348	0.0082	0.0030	0.0017	0.0011	0.0008
		R^2	0.9305	0.9807	0.9905	0.9909	0.9894	0.9876

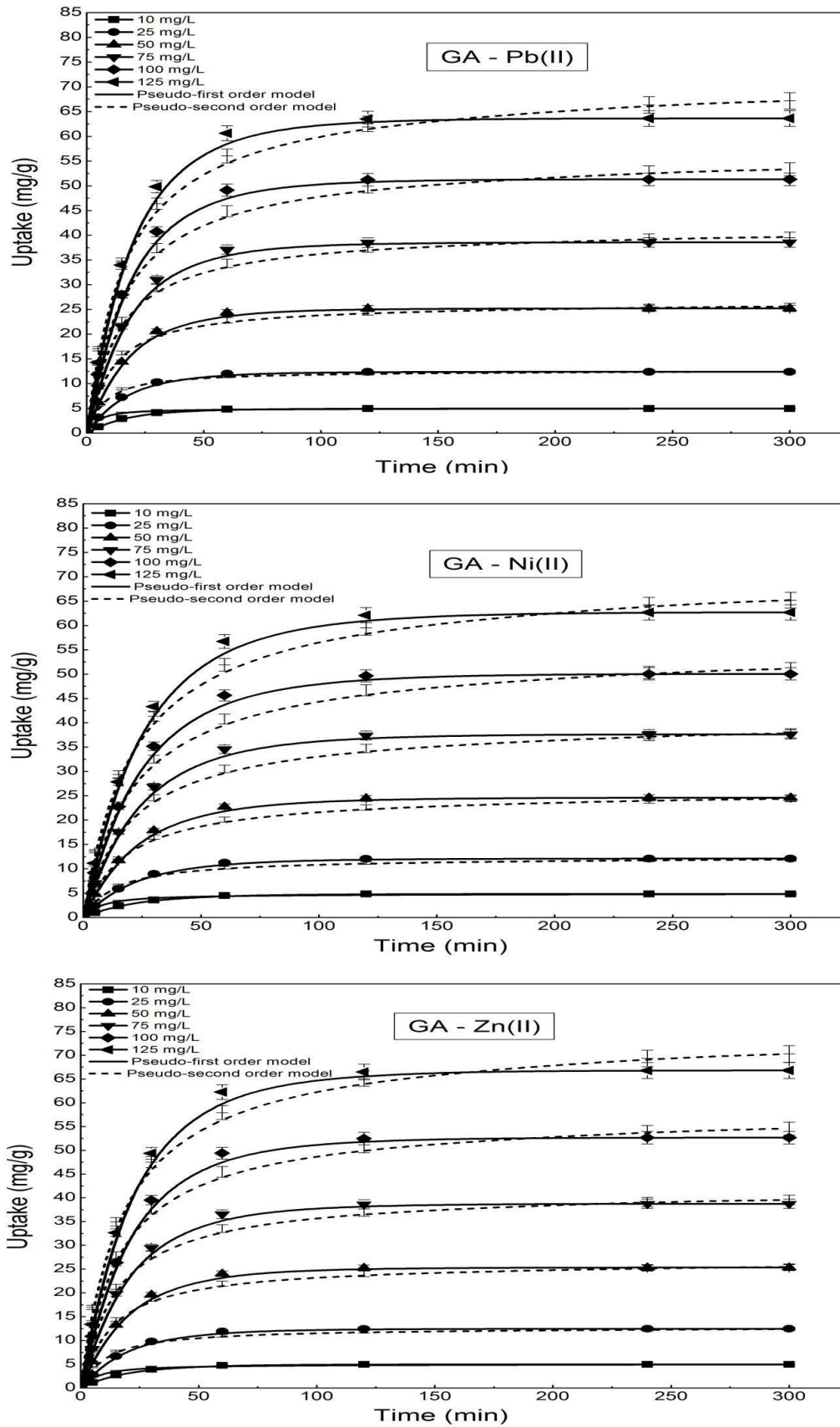


Fig. 6. Biosorption Kinetics of Pb(II), Ni(II), and Zn(II) onto *G. acerosa*.

Table 4
Comparison of present research work with previously published work

S. No	Adsorbent	Adsorbent capacity (mg/g)			Reference
		Pb	Ni	Zn	
1	Teakwood saw dust	NA	9.87	17.09	[47]
2	Groundnut shell	NA	7.49	9.57	[47]
3	Nigerian bamboo	17.50	7.50	27.50	[48]
4	Coconut shell	7.50	2.50	22.50	[48]
5	Pinus pinaster bark (pine tree)	1.59	NA	1.18	[49]
6	Tobacco dust	39.6	24.5	25.1	[50]
7	Mango peel	NA	39.75	28.21	[51]
8	Orange peel	7.75	6.01	5.25	[52]
9	Banana peel	7.97	6.88	5.8	[52]
10	Black gram husk	49.97	19.56	33.81	[53]
11	Peanut Husk	0.74	0.55	0.48	[54]
12	Pecan shell	64.2	NA	13.90	[55]
13	Coconut shells carbon	0.35	NA	0.39	[56]
14	Apricot stones carbon	0.36	NA	0.41	[56]
15	Peanut hulls	30	NA	9	[57]
16	Olive stone (microwaved AC)	23.47	12	15.08	[58]
17	Flax shive	87	19.2	18.2	[59]
18	Jute fibers	NA	5.26	5.95	[60]
19	Cabbage waste	61.27	NA	7.89	[61]
20	Coffee residues binding with clay	19.5	11	13.4	[62]
21	Olive mill solid residue	21.56	NA	5.4	[63]
22	Sesame straw biochar	102	NA	34	[64]
23	Peat moss	NA	14.69	13.27	[65]
24	Purolite biochar	37.8	NA	23.26	[66]
25	Purolite active carbon	29.2	NA	12.9	[66]
26	Waterworks sludge	20.41	NA	NA	[67]
27	Multiwall carbo nanotubes	26.54	NA	NA	[68]
28	Amberlite IR-120	19.20	NA	NA	[69]
29	Ti(IV) iodovanadate cation exchanger (TIV)	18.80	NA	NA	[70]
Sea species					
30	<i>Sargassum</i> sp.	0.62	0.96	1.51	[71]
31	<i>Ulva</i> sp.	1.55	7.89	7.96	[72]
32	<i>Ulva Lactuca</i>	54.30	NA	30	[73]
33	<i>Codium vermilara</i>	2.4	5.3	14.7	[74]
34	<i>Spirogyra insignis</i>	28	12.2	16.7	[74]
35	<i>Asparagopsis armata</i>	4.6	1.7	4.6	[74]
36	<i>Chondrus crispus</i>	4.1	6.6	4.8	[74]
37	<i>Fucus spiralis</i>	6.5	3.2	10.9	[74]
38	<i>Ascophyllum nodosum</i>	3	1.4	1.4	[74]
39	<i>Arthro bacter</i> sp.	130	13	NA	[75]
40	<i>Cystoseira indica</i>	47.22	7	NA	[76]
41	<i>Sargassum glaucescens</i>	45.84	6.35	NA	[76]
42	<i>Nizimuddinia zanardini</i>	50.41	6.38	NA	[76]
43	<i>Padina australis</i>	46.51	5.96	NA	[76]
44	<i>Sargassum</i> sp.	139.1	NA	29.8	[77]
45	<i>Laminaria hyperborea</i>	50.3	NA	19.2	[77]
46	<i>Sargassum muticum</i>	38.2	NA	34.1	[77]
47	<i>Fucus spiralis</i>	43.5	NA	34.3	[77]
48	<i>Bifurcaria bifurcata</i>	52.7	NA	30.3	[77]
49	<i>Padina</i> sp.	122.6	NA	35.1	[77]
50	<i>Aspergillus niger</i>	0.23	0.18	NA	[78]

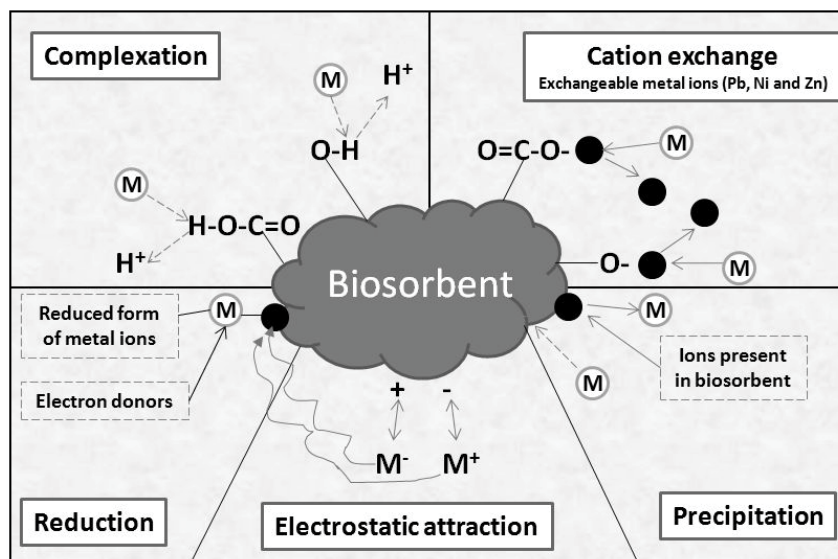


Fig. 7. Conceptual illustration of heavy metal sorption mechanisms onto the surface of biosorbent.

The kinetic data of three metal ions on *G. acerosa* was examined using pseudo-first- and pseudo-second-order models. These models focused on the premise that the rate of biosorption is equal to respectively the number of vacant sites on the biosorbent surface to the first and second power. The application of metal kinetics information to the pseudo-first-order model resulted in an outstanding forecast with a strong correlation coefficient (R^2) (Table 3). The model constants (Q_e and k_1) increased with the increase in initial metal concentration, indicating that high metal concentration favored the rate and quantity of biosorption. Similar to the measured experimental values, the model also expected uptake rates. In the event of pseudo-second-order kinetics (Table 3), the model over-predicted metal uptake rates along with relatively small R^2 . Fig. 6 provides the metal kinetic curve forecasts by two models compared to experimental kinetic data.

To understand the adsorption mechanism prediction of the rate-determining step is important. Commonly, solid-liquid adsorption is influenced by either external diffusion or intraparticle, or in some conditions both can happen. The adsorption mechanism can follow the three-step process as discussed below. First, it may be due to film diffusion, the movement of metals ions from the bulk solution to the external surface of the adsorbent. Second, it may be due to particle diffusion, metal ions will move to the interior to the adsorbents. Third, it may be adsorption, the metal ions move deep in the pores and binding spaces of the adsorbent [26]. A conceptual illustration of heavy metal sorption mechanisms on to the surface of biosorbent is given in Fig. 7. A comparison of present research work with previously published work is compared in Table 4.

3.6. Desorption studies

Desorption experiments were carried out to study the best elutant, solid to liquid ratio and regeneration cycles. Different elutants such as 0.1 M, HCl, H_2SO_4 , and HNO_3 and 0.1 $CaCl_2$ were used for the investigation [79]. For

Ni(II), 0.1 $CaCl_2$ is concluded as the best elutant with a maximum elution efficiency of 99.1% at an S/L ratio of 1 with three consecutive sorption elution cycles. Similarly, for Pb(II) and Zn(II), 0.1 M, HCl is concluded as the best elutant with a maximum elution efficiency of 99.2% and 99.3%. The S/L ratio of 1 and three sorption elution cycle is obtained for Pb(II) and Zn(II).

4. Conclusion

From this research, the following conclusion can be summarized:

- *G. acerosa*'s biosorption capability is heavily dependent on pH and sorbent dosage. Optimization studies show that peak metal uptake at pH 5, 2, and 8 corresponding to Pb(II), Ni(II), and Zn(II), and 2 g/L seaweed dosage has been attained.
- FT-IR, SEM, BET analyses proposed that the surfaces of *G. acerosa* seaweed could be affected by different functional groups with positive metal ions and better surface properties.
- Biosorption rates were discovered to be quick and equilibrium was achieved within 120 min. Applying metal ion kinetics data to the pseudo-first-order model led to excellent prediction over the pseudo-second-order model.
- Depending on the Langmuir model, the highest metal biosorption capability for Zn(II), Ni(II), and Pb(II) was recognized as 127.80, 87.82, and 73.99 mg/g, respectively.
- It can be found from these outcomes that *G. acerosa* seaweed has demonstrated a strong ability to behave as an effective and practical biosorbent to remove metal ions from wastewater.

References

- [1] D. Maiti, I. Ansari, M.A. Rather, A. Deepa, Comprehensive review on wastewater discharged from the coal-related

- industries - characteristics and treatment strategies, *Water Sci. Technol.*, 79 (2019) 2023–2035.
- [2] J. Jegan, S. Praveen, T. Bhagavathi Pushpa, R. Gokulan, Sorption kinetics and isotherm studies of cationic dyes using groundnut (*Arachis hypogaea*) shell derived biochar a low-cost adsorbent, *Appl. Ecol. Environ. Res.*, 18 (2020) 1925–1939.
 - [3] L. Zhang, Y. Zeng, Z. Cheng, Removal of heavy metal ions using chitosan and modified chitosan: a review, *J. Mol. Liq.*, 214 (2016) 175–191.
 - [4] T. Bhagavathi Pushpa, J. Vijayaraghavan, S.J. Sardhar Basha, V. Sekaran, K. Vijayaraghavan, J. Jegan, Investigation on removal of malachite green using EM based compost as adsorbent, *Ecotoxicol. Environ. Saf.*, 118 (2015) 177–182.
 - [5] G. Ravindiran, G.P. Ganapathy, J. Josephraj, A. Alagumalai, A critical insight into biomass derived biosorbent for bioremediation of dyes, *ChemistrySelect*, 4 (2019) 9762–9775.
 - [6] B. Pushpa T, J. Josephraj, P. Saravanan, G. Ravindran, Biodecolorization of basic blue 41 using EM based composts: isotherm and kinetics, *ChemistrySelect*, 4 (2019) 10006–10012.
 - [7] S. Praveen, T. Bhagavathi Pushpa, R. Gokulan, J. Jegan, Evaluation of the adsorption capacity of *Cocos nucifera* shell derived biochar for basic dyes sequestration from aqueous solution, *Energy Sources Part A*, (2020), doi: 10.1080/15567036.2020.1800142.
 - [8] M.K. Uddin, A review on the adsorption of heavy metals by clay minerals, with special focus on the past decade, *Chem. Eng. J.*, 308 (2017) 438–462.
 - [9] E. Vunain, A.K. Mishra, B.B. Mamba, Dendrimers, mesoporous silicas and chitosan-based nanosorbents for the removal of heavy-metal ions: a review, *Int. J. Biol. Macromol.*, 86 (2016) 570–586.
 - [10] A.T. Ojedokun, O.S. Bello, Sequestering heavy metals from wastewater using cow dung, *Water Resour. Ind.*, 13 (2016) 7–13.
 - [11] S. Srivastava, S.B. Agrawal, M.K. Mondal, A review on progress of heavy metal removal using adsorbents of microbial and plant origin, *Environ. Sci. Pollut. Res.*, 22 (2015) 15386–15415.
 - [12] A. Tripathi, M. Rawat Ranjan, Heavy metal removal from wastewater using low cost adsorbents, *J. Biorem. Biodegrad.*, 6 (2015) 1–5, doi: 10.4172/2155–6199.1000315.
 - [13] A. Ahmad, J.A. Siddique, M.A. Laskar, R. Kumar, S.H. Mohd-Setapar, A. Khatoun, R.A. Shiekh, New generation Amberlite XAD resin for the removal of metal ions: a review, *J. Environ. Sci.*, 31 (2015) 104–123.
 - [14] T. Babatunde Ibigbami, Removal of heavy metals from pharmaceutical industrial wastewater effluent by combination of adsorption and chemical precipitation methods, *Am. J. Appl. Chem.*, 4 (2016) 24–32.
 - [15] T. Bhagavathi Pushpa, J. Vijayaraghavan, K. Vijayaraghavan, J. Jegan, Utilization of effective microorganisms based water hyacinth compost as biosorbent for the removal of basic dyes, *Desal. Water Treat.*, 57 (2016) 24368–24377.
 - [16] R. Gokulan, G. Ganesh Prabhu, J. Jegan, A novel sorbent *Ulva lactuca*-derived biochar for remediation of Remazol Brilliant Orange 3R in packed column, *Water Environ. Res.*, 91 (2019) 642–649.
 - [17] J. Jegan, S. Praveen, T.B. Pushpa, R. Gokulan, Biodecolorization of Basic Violet 03 using biochar derived from agricultural wastes: isotherm and kinetics, *J. Biobased Mater. Bioenergy*, 14 (2020) 316–326.
 - [18] S. Siddique, K. Rovina, S. Al Azad, Heavy metal contaminants removal from wastewater using the potential filamentous fungi biomass: a review, *J. Microb. Biochem. Technol.*, 7 (2015) 384–393.
 - [19] M. Hua, S. Zhang, B. Pan, W. Zhang, L. Lv, Q. Zhang, Heavy metal removal from water/wastewater by nanosized metal oxides: a review, *J. Hazard. Mater.*, 211 (2012) 317–331.
 - [20] M. Fawzy, M. Nasr, S. Adel, S. Helmi, Regression model, artificial neural network, and cost estimation for biosorption of Ni(II)-ions from aqueous solutions by *Potamogeton pectinatus*, *Int. J. Phytorem.*, 20 (2018) 321–329.
 - [21] N. Suganthi, S.A. Nisha, S.K. Pandian, K.P. Devi, Evaluation of *Gelidiella acerosa*, the red algae inhabiting South Indian coastal area for antioxidant and metal chelating potential, *Biomed. Prev. Nutr.*, 3 (2013) 399–406.
 - [22] M.J. Ahmed, P.U. Okoye, E.H. Hummadi, B.H. Hameed, High-performance porous biochar from the pyrolysis of natural and renewable seaweed (*Gelidiella acerosa*) and its application for the adsorption of methylene blue, *Bioresour. Technol.*, 278 (2019) 159–164.
 - [23] M. Jamshidi, J. Keramat, N. Hamdami, O. Farhadian, Optimization of protein extraction from *Gelidiella acerosa* by carbohydrases using response surface methodology, *Phycol. Res.*, 66 (2018) 231–237.
 - [24] R. Gokulan, G.G. Prabhu, J. Jegan, Remediation of complex remazol effluent using biochar derived from green seaweed biomass, *Int. J. Phytorem.*, 21 (2019) 1179–1189.
 - [25] R. Gokulan, A. Avinash, G.G. Prabhu, J. Jegan, Remediation of remazol dyes by biochar derived from *Caulerpa scalpelliformis* - an eco-friendly approach, *J. Environ. Chem. Eng.*, 7 (2019) 103297, doi: 10.1016/j.jece.2019.103297.
 - [26] R. Gokulan, G. Ganesh Prabhu, A. Avinash, J. Jegan, Experimental and chemometric analysis of bioremediation of remazol dyes using biochar derived from green seaweeds, *Desal. Water Treat.*, 184 (2020) 340–353.
 - [27] A.M. Afzaal, Kinetics, isotherms and thermodynamics of heavy metal ions sorption onto raw and agro-based magnetic biosorbent, *Res. Adv. Environ. Sci.*, 1 (2018) 27–42.
 - [28] J. Jegan, J. Vijayaraghavan, T. Bhagavathi Pushpa, S.J. Sardhar Basha, Application of seaweeds for the removal of cationic dye from aqueous solution, *Desal. Water Treat.*, 57 (2016) 25812–25821.
 - [29] P. Senthil Kumar, S. Ramalingam, R.V. Abhinaya, K.V. Thiruvengadaravi, P. Baskaralingam, S. Sivanesan, Lead(II) adsorption onto sulphuric acid treated cashew nut shell, *Sep. Sci. Technol.*, 46 (2011) 2436–2449.
 - [30] D. Rangnani, R.K. Tak, Bio sorption of manganese(II) ions from aqueous solution by dry biomass of lantana camara, *Int. J. Green Herb. Chem.*, 6 (2017), 96–103.
 - [31] J. Thivya, J. Vijayaraghavan, Single and binary sorption of reactive dyes onto red seaweed-derived biochar: multi-component isotherm and modelling, *Desal. Water Treat.*, 156 (2019) 87–95.
 - [32] G.Z. Kyzas, M. Kostoglou, N.K. Lazaridis, D.N. Bikiaris, N-(2-Carboxybenzyl) grafted chitosan as adsorptive agent for simultaneous removal of positively and negatively charged toxic metal ions, *J. Hazard. Mater.*, 244 (2013) 29–38.
 - [33] W.S. Linghu, C. Wang, Adsorption of heavy metal ions from aqueous solution by chitosan, *Adv. Mater. Res.*, 881 (2014) 570–573.
 - [34] C. Ortiz-Calderon, H.C. Silva, D.B. Vásquez, Metal removal by seaweed biomass, *J.S. Tumuluru, Ed., Biomass Volume Estimation and Valorization for Energy*, IntechOpen, 2017. Available at: <https://www.intechopen.com/books/biomass-volume-estimation-and-valorization-for-energy/metal-removal-by-seaweed-biomass>
 - [35] J. Vijayaraghavan, T. Bhagavathi Pushpa, S.J. Sardhar Basha, J. Jegan, Isotherm, kinetics and mechanistic studies of methylene blue biosorption onto red seaweed *Gracilaria corticata*, *Desal. Water Treat.*, 57 (2015) 13540–13548.
 - [36] J. Thivya, J. Vijayaraghavan, Experimental and mathematical modelling of cationic dye sorption in up-flow packed column using *Gracilaria corticata*, *Desal. Water Treat.*, 167 (2019) 333–339.
 - [37] B.S. Journal, Lettuce leaves as biosorbent material to remove heavy metal ions from industrial wastewater, *Baghdad Sci. J.*, 11 (2014) 1164–1170.
 - [38] G. Neeraj, S. Krishnan, P. Senthil Kumar, K.R. Shriaishvarya, V. Vinoth Kumar, Performance study on sequestration of copper ions from contaminated water using newly synthesized high effective chitosan coated magnetic nanoparticles, *J. Mol. Liq.*, 214 (2016) 335–346.
 - [39] J. Vijayaraghavan, T. Bhagavathi Pushpa, S.J. Sardhar Basha, K. Vijayaraghavan, J. Jegan, Evaluation of red marine alga *Kappaphycus alvarezii* as biosorbent for methylene blue: isotherm, kinetic, and mechanism studies, *Sep. Sci. Technol.*, 50 (2014) 1120–1126.
 - [40] T.A. Khan, S.A. Chaudhry, I. Ali, Equilibrium uptake, isotherm and kinetic studies of Cd(II) adsorption onto iron oxide activated red mud from aqueous solution, *J. Mol. Liq.*, 202 (2015) 165–175.

- [41] I. Langmuir, The constitution and fundamental properties of solids and liquids. II. Liquids, *J. Am. Chem. Soc.*, 39 (1916) 1900–1950.
- [42] H.M.F. Freundlich, Adsorption in solution, *Z. Phys. Chem.*, 57 (1906) 385–471.
- [43] O. Redlich, D.L. Peterson, A useful adsorption isotherm, *J. Phys. Chem.*, 10 (1960) 1024, doi: 10.1021/j150576a611.
- [44] R. Sips, On the structure of a catalyst surface, *J. Chem. Phys.*, 16 (1948) 490–495.
- [45] S. Sagar, A. Rastogi, Evaluation of equilibrium isotherms and kinetic parameters for the adsorption of methyl orange dye onto blue green algal biomass, *Asian J. Chem.*, 31 (2019) 1501–1508.
- [46] J. Ayorinde, J.E. Osula, Isotherm, kinetic and thermodynamic studies of Pb(II) and nickel ions removal from aqueous solution using locally sourced bio-adsorbent, *Int. J. Mater. Sci. Eng.*, 7 (2019) 67–80.
- [47] S.S. Shukla, L.J. Yu, K. Dorris, A. Shukla, Removal of nickel from aqueous solutions by sawdust, *J. Hazard. Mater.*, 121 (2005) 243–246.
- [48] F.T. Ademiluyi, E.O. David-West, Effect of chemical activation on the adsorption of heavy metals using activated carbons from waste materials, *ISRN Chem. Eng.*, 2002 (2012) 1–5, doi: 10.5402/2012/674209.
- [49] G. Vázquez, G. Antorrena, J. González, M.D. Doval, Adsorption of heavy metal ions by chemically modified *Pinus pinaster* bark, *Bioresour. Technol.*, 48 (1994) 251–255.
- [50] B.C. Qi, C. Aldrich, Biosorption of heavy metals from aqueous solutions with tobacco dust, *Bioresour. Technol.*, 99 (2008) 5595–5601.
- [51] M. Iqbal, A. Saeed, I. Kalim, Characterization of adsorptive capacity and investigation of mechanism of Cu²⁺, Ni²⁺ and Zn²⁺ adsorption on mango peel waste from constituted metal solution and genuine electroplating effluent, *Sep. Sci. Technol.*, 44 (2009) 3770–3791.
- [52] G. Annadurai, R.S. Juang, D.J. Lee, Adsorption of heavy metals from water using banana and orange peels, *Water Sci. Technol.*, 47 (2003) 185–190.
- [53] A. Saeed, M. Iqbal, Bioremoval of cadmium from aqueous solution by black gram husk (*Cicer arietinum*), *Water Res.*, 37 (2003) 3472–3480.
- [54] K. Wilson, H. Yang, C.W. Seo, W.E. Marshall, Select metal adsorption by activated carbon made from peanut shells, *Bioresour. Technol.*, 97 (2006) 2266–2270.
- [55] R.R. Bansode, J.N. Losso, W.E. Marshall, R.M. Rao, R.J. Portier, Adsorption of metal ions by pecan shell-based granular activated carbons, *Bioresour. Technol.*, 89 (2003) 115–119.
- [56] M.M. Rahman, M. Adil, A.M. Yusof, Y.B. Kamaruzzaman, R.H. Ansary, Removal of heavy metal ions with acid activated carbons derived from oil palm and coconut shells, *Materials*, 60 (1994) 177–182.
- [57] P. Brown, I. Atly Jefcoat, D. Parrish, S. Gill, E. Graham, Evaluation of the adsorptive capacity of peanut hull pellets for heavy metals in solution, *Adv. Environ. Res.*, 4 (2000) 19–29.
- [58] T.M. Alslaibi, I. Abustan, M.A. Ahmad, A.A. Foul, Application of response surface methodology (RSM) for optimization of Cu²⁺, Cd²⁺, Ni²⁺, Pb²⁺, Fe²⁺, and Zn²⁺ removal from aqueous solution using microwaved olive stone activated carbon, *J. Chem. Technol. Biotechnol.*, 88 (2013) 2141–2151.
- [59] E.I. El-Shafey, M. Cox, A.A. Pichugin, Q. Appleton, Application of a carbon sorbent for the removal of cadmium and other heavy metal ions from aqueous solution, *J. Chem. Technol. Biotechnol.*, 77 (2002) 429–436.
- [60] S.R. Shukla, R.S. Pai, Adsorption of Cu(II), Ni(II) and Zn(II) on modified jute fibres, *Bioresour. Technol.*, 96 (2005) 1430–1438.
- [61] M.A. Hossain, H.H. Ngo, W.S. Guo, L.D. Nghiem, F.I. Hai, S. Vigneswaran, T.V. Nguyen, Competitive adsorption of metals on cabbage waste from multi-metal solutions, *Bioresour. Technol.*, 160 (2014) 79–88.
- [62] V. Boonamnuayvitaya, C. Chaiya, W. Tanthapanichakoon, S. Jarudilokkul, Removal of heavy metals by adsorbent prepared from pyrolyzed coffee residues and clay, *Sep. Purif. Technol.*, 35 (2004) 11–22.
- [63] S.H. Gharaibeh, W.Y. Abu-El-Sha'r, M.M. Al-Kofahi, Removal of selected heavy metals from aqueous solutions using processed solid residue of olive mill products, *Water Res.*, 32 (1998) 498–502.
- [64] J.H. Park, Y.S. Ok, S.H. Kim, J.S. Cho, J.S. Heo, R.D. Delaune, D.C. Seo, Competitive adsorption of heavy metals onto sesame straw biochar in aqueous solutions, *Chemosphere*, 142 (2016) 77–83.
- [65] M. Adeli, Y. Yamini, M. Faraji, Removal of copper, nickel and zinc by sodium dodecyl sulphate coated magnetite nanoparticles from water and wastewater samples, *Arabian J. Chem.*, 28 (1993) 1261–1276.
- [66] D. Kołodźńska, J. Krukowska, P. Thomas, Comparison of sorption and desorption studies of heavy metal ions from biochar and commercial active carbon, *Chem. Eng. J.*, 307 (2017) 353–363.
- [67] A.A.H. Faisal, S.F.A. Al-Wakel, H.A. Assi, L.A. Naji, M. Naushad, Waterworks sludge-filter sand permeable reactive barrier for removal of toxic lead ions from contaminated groundwater, *J. Water Process Eng.*, 33 (2020) 1–11, doi: 10.1016/j.jwpe.2019.101112.
- [68] A. Mittal, M. Naushad, G. Sharma, Z.A. Allothman, S.M. Wabaidur, M. Alam, Fabrication of MWCNTs/ThO₂ nanocomposite and its adsorption behavior for the removal of Pb(II) metal from aqueous medium, *Desal. Water Treat.*, 57 (2015) 21863–21869.
- [69] M. Naushad, Z.A. AlOthman, Separation of toxic Pb²⁺ metal from aqueous solution using strongly acidic cation-exchange resin: analytical applications for the removal of metal ions from pharmaceutical formulation, *Desal. Water Treat.*, 53 (2013) 2158–2166.
- [70] M. Naushad, Z.A. AlOthman, M.R. Awual, M.M. Alam, G.E. Eldesoky, Adsorption kinetics, isotherms, and thermodynamic studies for the adsorption of Pb²⁺ and Hg²⁺ metal ions from aqueous medium using Ti(IV) iodovanadate cation exchanger, *Ionics*, 21 (2015) 2237–2245.
- [71] K. Vijayaraghavan, U.M. Joshi, S. Kamala-Kannan, An attempt to develop seaweed-based treatment technology for the remediation of complex metal-bearing laboratory wastewaters, *Ecol. Eng.*, 47 (2012) 278–283.
- [72] K. Vijayaraghavan, U.M. Joshi, R. Balasubramanian, Removal of metal ions from storm-water runoff by low-cost sorbents: batch and column studies, *J. Environ. Eng.*, 136 (2010) 1113–1118.
- [73] M.M. Areco, S. Hanel, J. Duran, M. dos Santos Afonso, Biosorption of Cu(II), Zn(II), Cd(II) and Pb(II) by dead biomasses of green alga *Ulva lactuca* and the development of a sustainable matrix for adsorption implementation, *J. Hazard. Mater.*, 213–214 (2012) 123–132.
- [74] A. Leusch, Z.R. Holan, B. Volesky, Biosorption of heavy metals (Cd, Cu, Ni, Pb, Zn) by chemically reinforced biomass of marine algae, *J. Chem. Technol. Biotechnol.*, 62 (1995) 279–288.
- [75] F. Veglió, F. Beolchini, A. Gasbarro, Biosorption of toxic metals: an equilibrium study using free cells of *Arthrobacter* sp., *Process Biochem.*, 32 (1997) 99–105.
- [76] M.M. Montazer-Rahmati, P. Rabbani, A. Abdolali, A.R. Keshtkar, Kinetics and equilibrium studies on biosorption of cadmium, lead, and nickel ions from aqueous solutions by intact and chemically modified brown algae, *J. Hazard. Mater.*, 185 (2011) 401–407.
- [77] O.M.M. Freitas, R.J.E. Martins, C.M. Delerue-Matos, R.A.R. Boaventura, Removal of Cd(II), Zn(II) and Pb(II) from aqueous solutions by brown marine macro algae: kinetic modelling, *J. Hazard. Mater.*, 153 (2008) 493–501.
- [78] P. Pavasant, R. Apiratikul, V. Sungkhum, P. Suthiparinyanont, S. Wattanachira, T.F. Marhaba, Biosorption of Cu²⁺, Cd²⁺, Pb²⁺, and Zn²⁺ using dried marine green macroalga *Caulerpa lentillifera*, *Bioresour. Technol.*, 97 (2006) 2321–2329.
- [79] G. Ravindiran, R.M. Jeyaraju, J. Josephraj, A. Alagumalai, Comparative desorption studies on remediation of remazol dyes using biochar (sorbent) derived from green marine seaweeds, *ChemistrySelect*, 4 (2019) 7437–7445.